博士学位論文

放射線治療のための万能ボーラスの開発と評価

近畿大学大学院
医学研究科医学系専攻

中　村　憲　治

Doctoral Dissertation

The development and characterization of an all-purpose bolus for radiotherapy

November 2023

Major in Medical Sciences
Kindai University Graduate School of Medical Sciences

Kenji Nakamura

課博

同　意　書

2023 年 10 月 17 日

近畿大学大学院
医学研究科長　殿

共著者　門前 一　印　　共著者　久保和輝　印

共著者　小坂浩之　印　　共著者　伊藤崇晃　印

共著者　酒井優佑　印　　共著者　柳　勇也　印

共著者　西村恭昌　印　　共著者　　印

共著者　　印　　共著者　　印

論文題目

The development and characterization of an all-purpose bolus for radiotherapy

下記の博士論文提出者が、標記論文を貴学医学博士の学位論文（主論文）として使用することに同意いたします。

また、標記論文を再び学位論文として使用しないことを誓約いたします。

記

1．博士論文提出者氏名　　中村　憲治

2．専攻分野　　医学系　　医学物理学

近畿大学大学院医学研究科

The development and characterization of an all-purpose bolus for radiotherapy

Kenji Nakamura[1, 2], Hajime Monzen[1*], Kazuki Kubo[1], Hiroyuki Kosaka[1], Takaaki Ito[1], Yusuke Sakai[1, 2], Yuya Yanagi[1], Yasumasa Nishimura[3]

1. Department of Medical Physics, Graduate School of Medical Sciences, Kindai University, 377-2, Onohigashi, Osakasayama, Osaka, 589-8511, Japan

2. Department of Radiotherapy, Takarazuka City Hospital, 4-5-1, Kohama, Takarazuka, Hyogo, 665-0827, Japan

3. Department of Radiation Oncology, Faculty of Medicine, Kindai University, 377-2, Onohigashi, Osakasayama, Osaka, 589-8511, Japan

* Corresponding author:

Hajime Monzen, Ph.D.

Department of Medical Physics, Graduate School of Medical Sciences, Kindai University

377-2 Onohigashi, Osakasayama, Osaka, Japan

TEL: +81-72-366-0221 FAX: +81-72-365-7161

E-mail: hmon@med.kindai.ac.jp

Abstract

Objective. The purpose of this study was to develop a new bolus (HM bolus), with tissue equivalence, transparency, reusability, and free shaping at approximately 40 °C for excellent adhesion, and to evaluate the feasibility of clinically using this bolus as an ideal bolus. *Approach.* We summarized the advantages and disadvantages of existing boluses. To evaluate dose characteristics, a vinyl gel sheet bolus (Gel bolus) and HM bolus placed on a water-equivalent phantom were used to obtain the percent depth dose (PDD) of electron (6 MeV, 9 MeV) and photon (4 MV, 6 MV) beams. The average dose difference of the HM bolus and Gel bolus was calculated. The Gel bolus, a soft rubber bolus (SR bolus), and HM bolus were placed in adherence to a pelvic phantom. CT images taken after shaping and 1, 2, and 3 weeks after shaping were used to evaluate the adhesion and reproducibility using air gap and dice similarity coefficient (DSC). *Main results.* The average dose difference for electron beams was 0.16% ± 0.79% and photon beams was 0.06% ± 0.34%, both within 1% of the PDD results. The HM bolus showed the same build-up effect and dose characteristics as the Gel bolus. The mean air gap values for the Gel bolus, SR bolus, and HM bolus were 96.02 ± 43.77 cm^3, 34.93 ± 21.44 cm^3, and 4.40 ± 1.50 cm^3, respectively. The mean DSC values compared to initial images for the Gel bolus, SR bolus, and HM bolus were 0.363 ± 0.035, 0.556 ± 0.042, and 0.837 ± 0.018, respectively. Excellent adhesion was observed in the CT simulation and during the treatment period. *Significance.* The HM bolus has unique features, such as tissue equivalence, transparency, reusability, and free shaping for excellent adhesion, and is thus an ideal bolus for use in clinical cases.

Key words: bolus, radiotherapy, free shaping, adhesion, transparency

1. Introduction

The ideal bolus properties include strong adhesion to the patient, ability to shape in real time without requiring high pressure on the patient, no change in beam characteristics after bolus transmission, transparency, reusability, tissue equivalence and accurate calculation by the treatment planning system (TPS), and sufficient and uniform thickness for build-up. Various boluses have advantages and disadvantages (ICRU 1989, Vyas et al 2013, Fagerstrom 2019, Richmond et al 2016, Al-Rahbi et al 2018, Canters et al 2016, Fujimoto et al 2017, Baltz et al 2019, Park et al 2019), and Aoyama et al. noted that there is no bolus that currently meets all of the conditions (Aoyama et al 2020). In the past few years, newly developed boluses with unique features have been reported from all over the world (Al-Sudani et al 2020, Sakai et al 2021, Okuhata et al 2021, Muramatsu et al 2021, Wakabayashi et al 2021, Chatchumnan et al 2022, Wang et al 2022).

Boluses, especially those used in external radiation therapy for superficial tumors, are used to deliver an adequate dose to the skin surface (Recht et al 2001, Kudchadker et al 2003, Khan and Gibbons 2014). Previous studies have reported that the air layer between the bolus and body surface affects the dose distribution when the bolus does not sufficiently adhere to the unevenness of the body surface (Sharma and Johnson 1993, Behrens 2006, Kong and Holloway 2007). The influence is observed especially for electron beams (Kong and Holloway 2007) or more importantly, air gaps of several cm (Behrens 2006). The vinyl gel sheet bolus (Gel bolus) (ICRU 1989), the most versatile bolus in clinical use, is inexpensive, reusable, and guarantees a stable build-up effect with tissue equivalents; however, the Gel bolus has problems such as difficulty in adhering to uneven body surfaces

including head and neck tumors and the chest wall after a mastectomy (Boman et al 2018, Lobo et al 2020). A thermoplastic shell bolus shows the same build-up effect as the Gel bolus and has advantages in terms of patient immobilization (Fagerstrom 2019, Sakai et al 2021); however, because the material is hard at room temperature, it is difficult to adhere to areas with deep grooves such as the outer ear and vulva. Additionally, the hardness of a plastic bolus may cause discomfort to patients with sensitive skin or open wounds. A high atomic number bolus has sufficient build-up effects and excellent adhesion in a few areas; however, it is not a tissue-equivalent material, which has disadvantages for accurate dose calculations in TPS (Richmond et al 2016, Al-Rahbi et al 2018, Okuhata et al 2021). A 3D printed bolus is made of a tissue-equivalent material and has been used with excellent adhesion to a variety of sites (Canters et al 2016, Fujimoto et al 2017, Baltz et al 2019, Chatchumnan et al 2022, Wang et al 2022). Furthermore, Park et al. developed Dragon Skin, which has excellent adhesion during CT simulation and in clinical practice (Park et al 2019). Alternatively, 3D printed boluses have disadvantages in terms of transparency, reusability, and real-time molding. It is clinically important to develop a bolus that has the advantages of these previous materials but without their disadvantages.

The purpose of this study was to develop a new bolus that satisfies all of the ideal bolus conditions for clinical use. The advantages of the new bolus were clarified in comparison with the characteristics of other boluses.

2. Materials and methods

Table 1 summarizes the advantages and disadvantages of boluses in previous

studies evaluated on a three-point scale: good (○) for characteristics that have been clarified as features or advantages, poor (×) for characteristics that have been clarified as limitations or disadvantages, and unclear (-) for characteristics that have not been described or discussed.

Table 1. The advantages and disadvantages of each bolus evaluated on the three-point scale as good: ○, poor: ×, unclear: -.

	Tissue equivalence (dose calculable)	Transparency	Sufficient thickness for build-up	Adhesion (CT simulation)	Adhesion (each treatment)	Shaping in real-time	Reusability
Gel bolus (ICRU 1989)	○	○	○	×	×	-	○
Thermoplastic shell bolus (Fagerstrom 2019, Sakai et al 2021)	○	×	○	○	-	-	×
High atomic number bolus (Richmond et al 2016, Al-Rahbi et al 2018, Okuhata et al 2021)	×	×	○	○	-	-	○
3D printed bolus (Canters et al 2016, Fujimoto et al 2017, Baltz et al 2019)	○	×	○	○	-	-	×
Dragon Skin (Park et al 2019)	○	×	○	○	○	-	×
Shape memory bolus (Aoyama et al 2020)	○	○	×	○	-	○	○
Soft Rubber bolus (Wakabayashi et al 2021)	○	×	○	○	-	○	○

2.1. Physical characteristics of a new bolus

The newly developed bolus was controlled to prevent phase separation by adjusting the contents of ethylene propylene rubber, styrene, butadiene rubber, thermoplastic resin, temperature-sensitive adjuster, and silica. We named this new bolus the HM bolus. The element ratios (wt%) in the HM bolus are H: 10.2%, C:

63.5%, O: 17.1%, and Si: 9.2%. The density was adjusted to 0.96 g cm^{-3}.

The product was optimized to enable free shaping at 40 °C without requiring high pressure to avoid discomfort to patients with sensitive or open skin. The viscoelasticity of the new bolus was changed with heating; therefore, a dynamic mechanical analysis (DMA) was performed to clarify its response to temperature. Figure 1 shows the DMA procedure. The DMA equipment was calibrated every morning by trained professional engineers. The calibration was performed by recognizing and initially setting the gripper's moving parts and stress detectors without the test material attached to the measurement section.

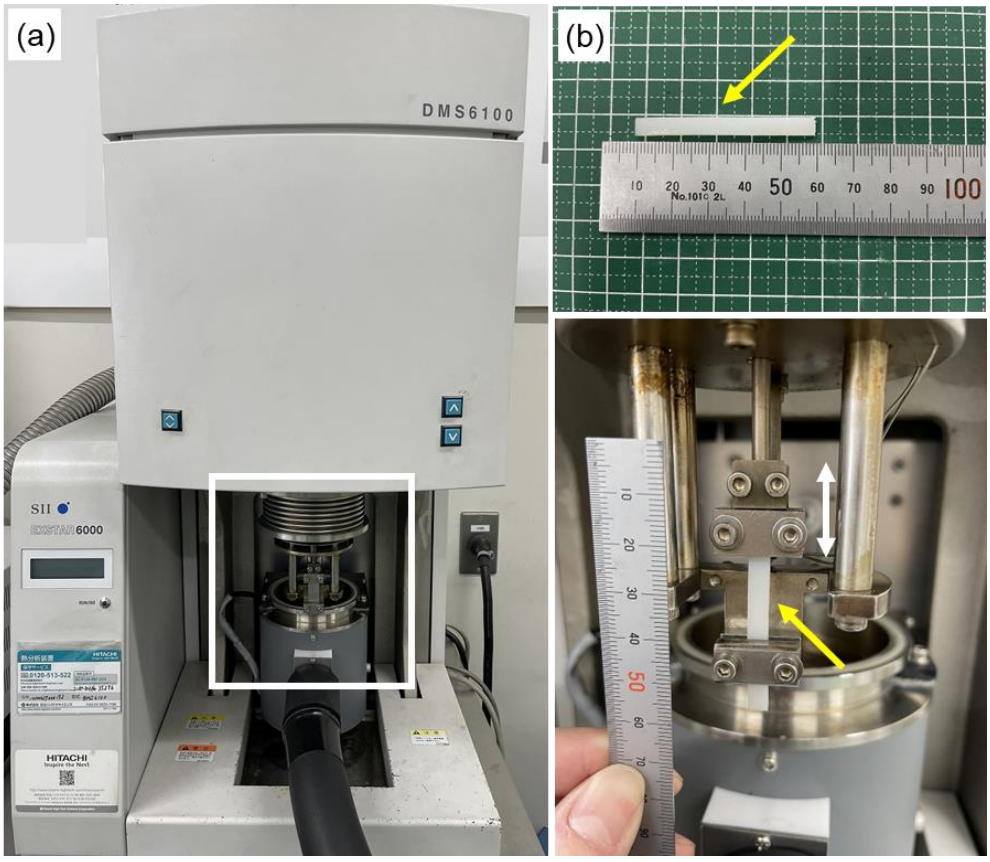

Figure 1. (a) Measuring equipment (DMS6100; HITACHI high-tech, Tokyo, Japan). The white box indicates the measurement section. (b) The yellow arrow points to the test material. The size of the sample is width = 5 mm, length = 50 mm, thickness = 2 mm. The white sample is for visibility. (c) Enlarged measurement section. The stresses for minute fluctuations of the gripper in the direction of both

arrows are measured at each temperature.

The following three parameters are used to define the elastic properties of the HM bolus: the storage modulus (E') is related to elasticity, loss modulus (E") is related to viscosity, and the ratio of the moduli (E"/E') is defined as tan δ. A high tan δ value means high viscosity, while a low tan δ means high elasticity (Wakabayashi et al 2021, Geethamma et al 1995, Monzen et al 2019).

Figure 2 shows the DMA of the HM bolus, which can be freely shaped when tan δ is greater than 0.46, corresponding to the temperature of 41.1 °C. Tan δ was adjusted to 0.20, corresponding to room temperature (assumed to be 20 °C), to maintain high shape retention in storage.

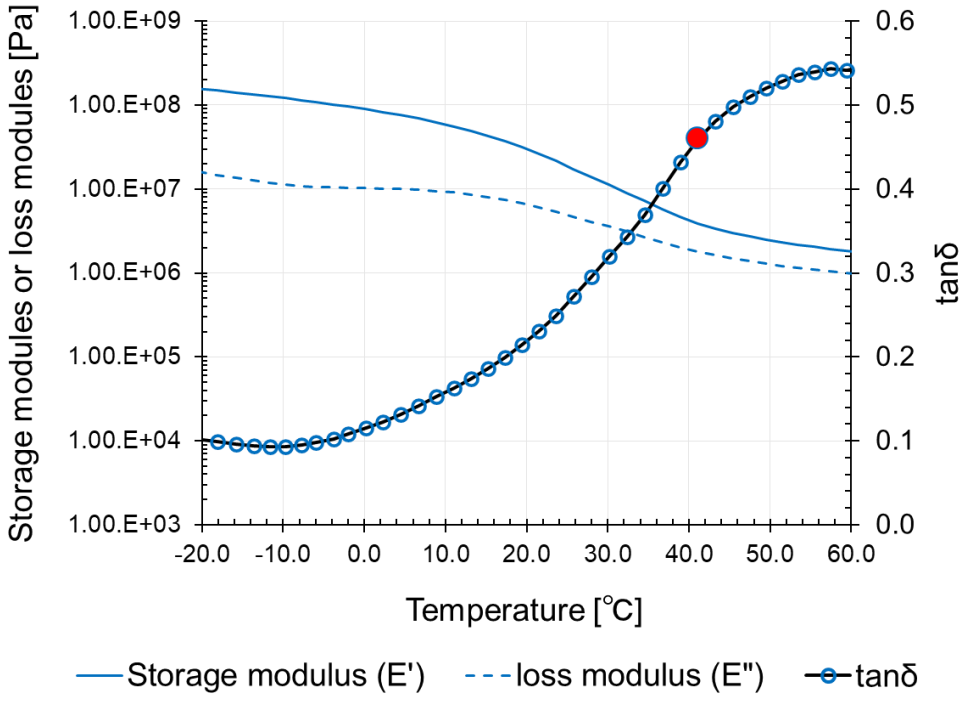

Figure 2. Dynamic mechanical analysis clarifying the temperature-dependent viscoelastic properties of the HM bolus. The storage modulus (E') is related to elasticity, loss modulus (E") is related to viscosity, and the ratio of the moduli (E"/E') is defined as tan δ. The red dot shows the freely shaping temperature

(41.1 °C).

2.2. Dosimetric evaluation using a water-equivalent phantom

To evaluate the dose characteristics, a bolus was placed on a water-equivalent phantom (Tough Water Phantom; Kyoto Kagaku Co., Ltd., Kyoto, Japan). A parallel-plate ionization chamber (Roos Type 34001; PTW, Freiburg, Germany) and a RAMTEC Duo electrometer (Toyo Medic, Tokyo, Japan) were used to obtain the percent depth dose (PDD) of electron (6 MeV, 9 MeV) and photon (4 MV, 6 MV) beams from the TrueBeam (Varian Medical Systems, Palo Alto, CA, USA). The HM bolus was compared with a Gel bolus (Bolx-I, CIVCO Medical Solution, Orange City, IA, USA). For both HM and Gel boluses, the size was 30 cm × 30 cm and the diameter was 5 mm. The source to surface distance (SSD) was 100 cm, the field size was 10 cm × 10 cm, and irradiation was performed at 200 monitor units (MU) (Figure 3) (Wakabayashi et al 2021, Adamson et al 2017). The dose difference between the Gel bolus and HM bolus was calculated at depths of 0, 3, 15, and 30 mm for the electron beam and 0, 15, 50, and 100 mm for the photon beam using Equation 1. All standard deviations (SD) in this paper are expressed as ± 1 SD.

$$Dose\ \ Difference\ \ (\%) = \frac{HM\ \ bolus\ \ dose - Gel\ \ bolus\ \ dose}{Gel\ \ bolus\ \ dose} \times 100 \qquad (1)$$

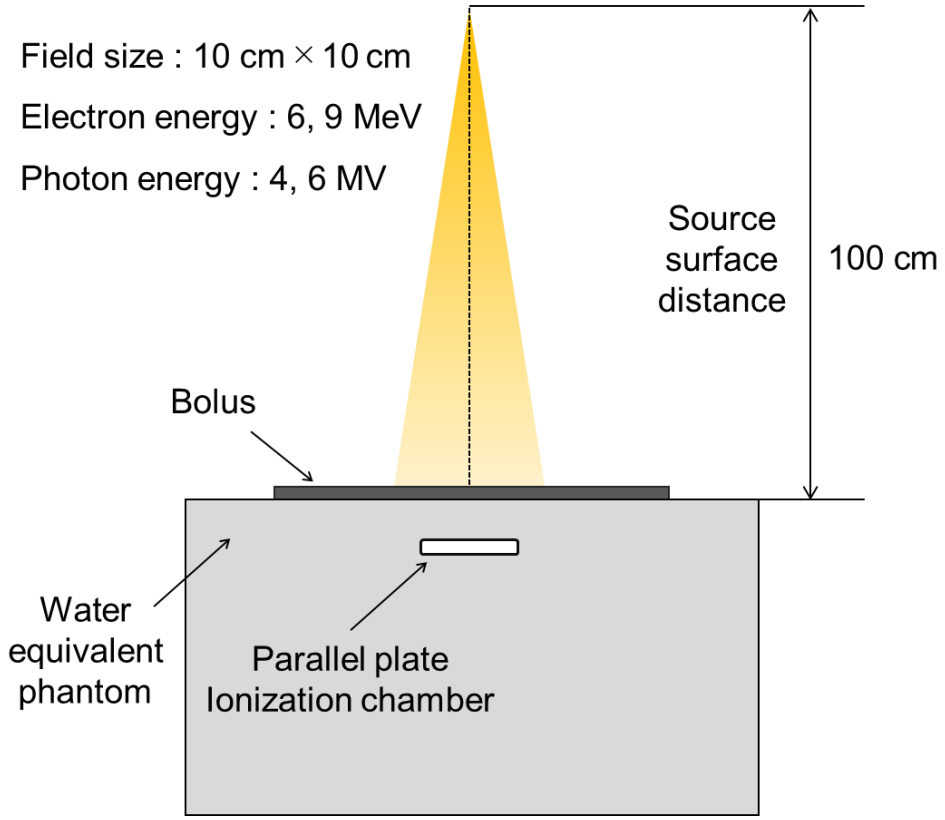

Figure 3. Schematics of the experimental geometries for percentage depth dose.

2.3. Evaluation of the adhesion and reproducibility of the bolus at three points

A pelvic phantom (BrainLab AG, Feldkirchen, Germany) was used to evaluate the adhesion and reproducibility of the Gel bolus, soft rubber bolus (SR bolus) (Wakabayashi et al 2021), and HM bolus on uneven body surfaces. The SR bolus and HM bolus were heated at 60°C for 5 min using a RapidHeat™ Oven (Q-Fix, Inc. Avondale, PA, USA), then shaped and adhered to the phantom from the lower abdomen to the crotch (Figure 4). We used the RapidHeat Oven for this study because the temperature (lower limit: 60 °C, upper limit: 80 °C) and heating time can be set without subjectivity.

The images were acquired using the Aquilion LB CT system (Canon Medical Systems, Tochigi, Japan) and transferred to MIM Maestro software (version 7.2.3, MIM Software Inc, Cleveland, OH, USA) (MIM). Imaging conditions were as

follows: tube voltage = 120 kV, tube current = 500 mA, matrix size = 512 × 512 pixels, field of view = 400 mm, and slice thickness = 2 mm. First, the SR and HM boluses were set to let a thing alone for 3 weeks without reheating, and the air gap determined by CT imaging was compared. Second, each bolus was set up, shaped on the phantom, and imaged immediately after shaping and at 1, 2, and 3 weeks after shaping. The SR and HM boluses were reheated at 60 °C (lower limit) for 20 s using the RapidHeat Oven before it was placed on the phantom to anticipate cases of anatomical modifications of the patient surface. We chose 20 s because the bolus was not viscous after it was reheated at 60 °C for 10 s, and the bolus could not maintain its shape after it was reheated at 60 °C for 30 s.

The phantom and bolus were contoured using MIM, and the air layer between the bolus and phantom from the top of the pubic symphysis to the bottom of the ischium was identified with a threshold of −500 HU, and this volume was defined as the air gap (Nakano et al 2013). To evaluate the stability of the density inside the bolus over time and reheat, the mean CT value (HU) at each time point was examined. Furthermore, the reproducibility of the bolus 1, 2, and 3 weeks after shaping compared with just after shaping was evaluated using the dice similarity coefficient (DSC) (Dice 1945). The DSC was calculated using Equation 2.

$$DSC = \frac{2(A \cap B)}{A + B} \tag{2}$$

DSC values range from 0 to 1, with a higher DSC indicating a higher degree of similarity between any two sets. All DSC values were automatically analyzed using MIM.

The visibility of letters (maximum: 80 pt, minimum: 10 pt) through a plate-shaped bolus and the visibility of markers when each bolus was set up on the pelvic

phantom under normal room lighting were evaluated (Adamson et al 2017).

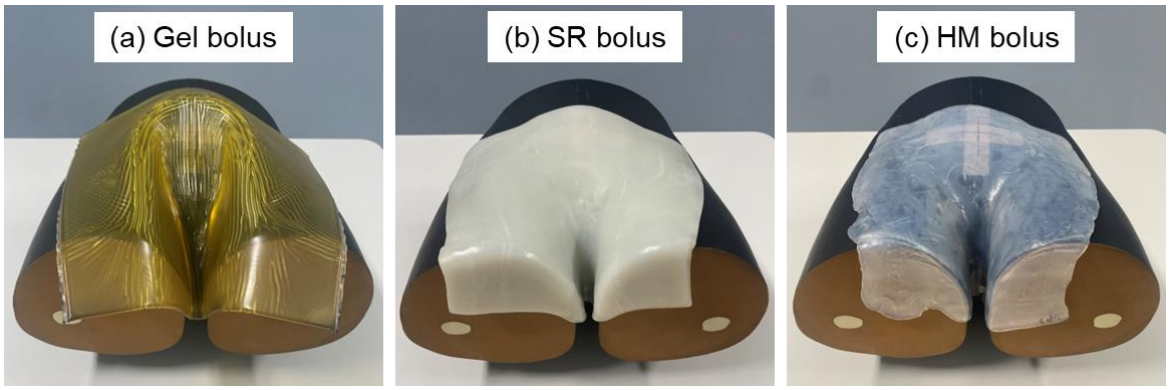

Figure 4. Each bolus was adhered to the pelvic phantom from the lower abdomen to the crotch.

3. Results

3.1. Dosimetric evaluation using the water-equivalent phantom

Figure 5 shows the PDD of the Gel bolus and HM bolus in electron beams (6 MeV, 9 MeV) and photon beams (4 MV, 6 MV). The average dose difference for electron beams up to a depth of 50 mm was 0.16% ± 0.79%, and that for photon beams up to a depth of 200 mm was 0.06% ± 0.34%, both within 1%. The HM bolus showed the same build-up effect and dose characteristics as the Gel bolus in electron beams (6 MeV, 9 MeV) and photon beams (4 MV, 6 MV).

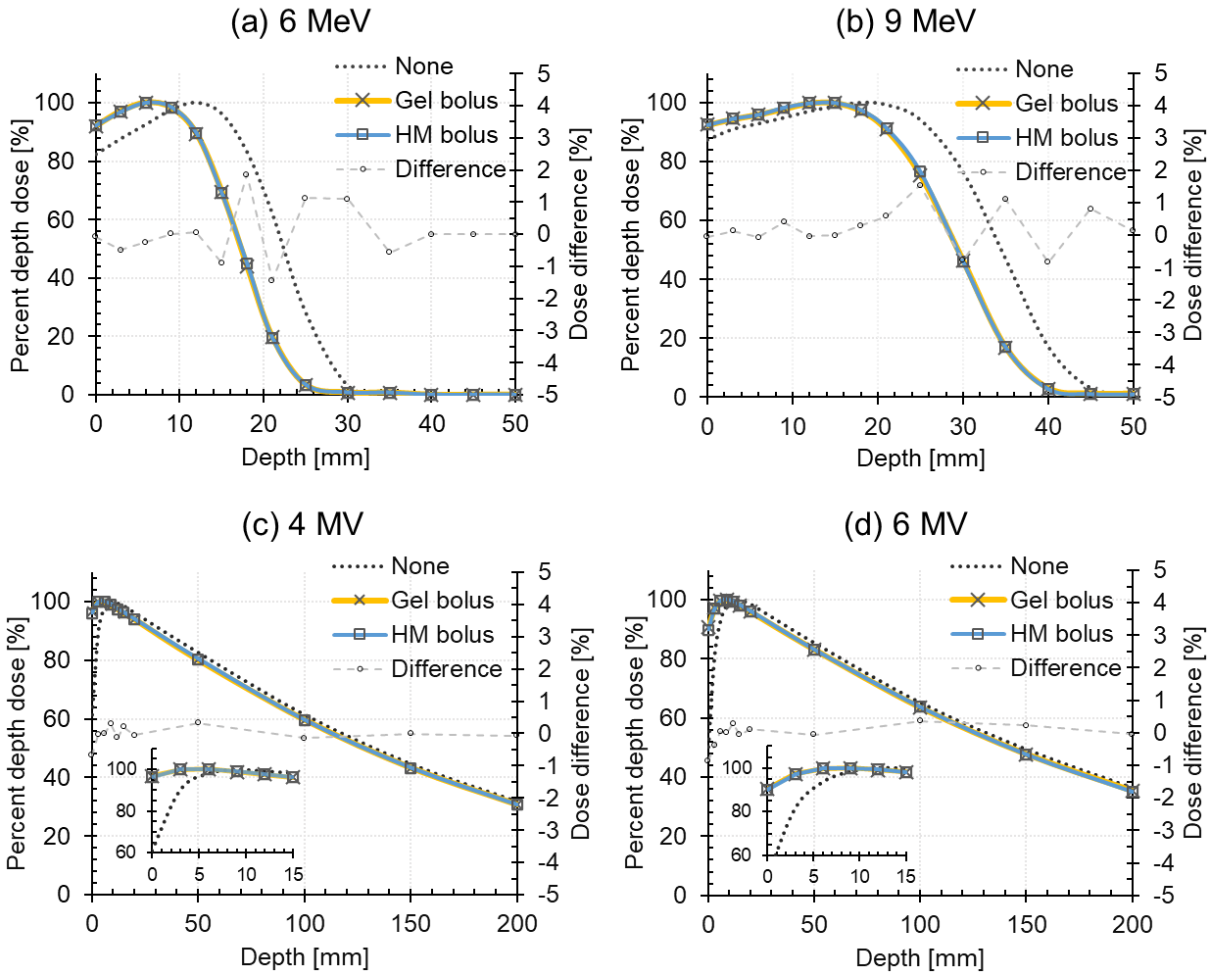

Figure 5. Comparison of the percentage depth dose of (a) 6 MeV and (b) 9 MeV electron beams and (c) 4 MV and (d) 6 MV photon beams for the Gel bolus and HM bolus. The second axis shows the dose difference between the Gel and HM boluses.

3.2. Evaluation of the adhesion and reproducibility of the bolus at three time points

Figure 6 shows images of the SR and HM boluses just after shaping, left for 3 weeks, and then reheated. A transverse image of the lower edge of the ischium is displayed with a window level of −400 HU and a window width of 1300 HU. Compared with the HM bolus without reheating, the HM bolus with reheating showed superior adhesion and reproducibility. No effect of reheating on the SR bolus was observed.

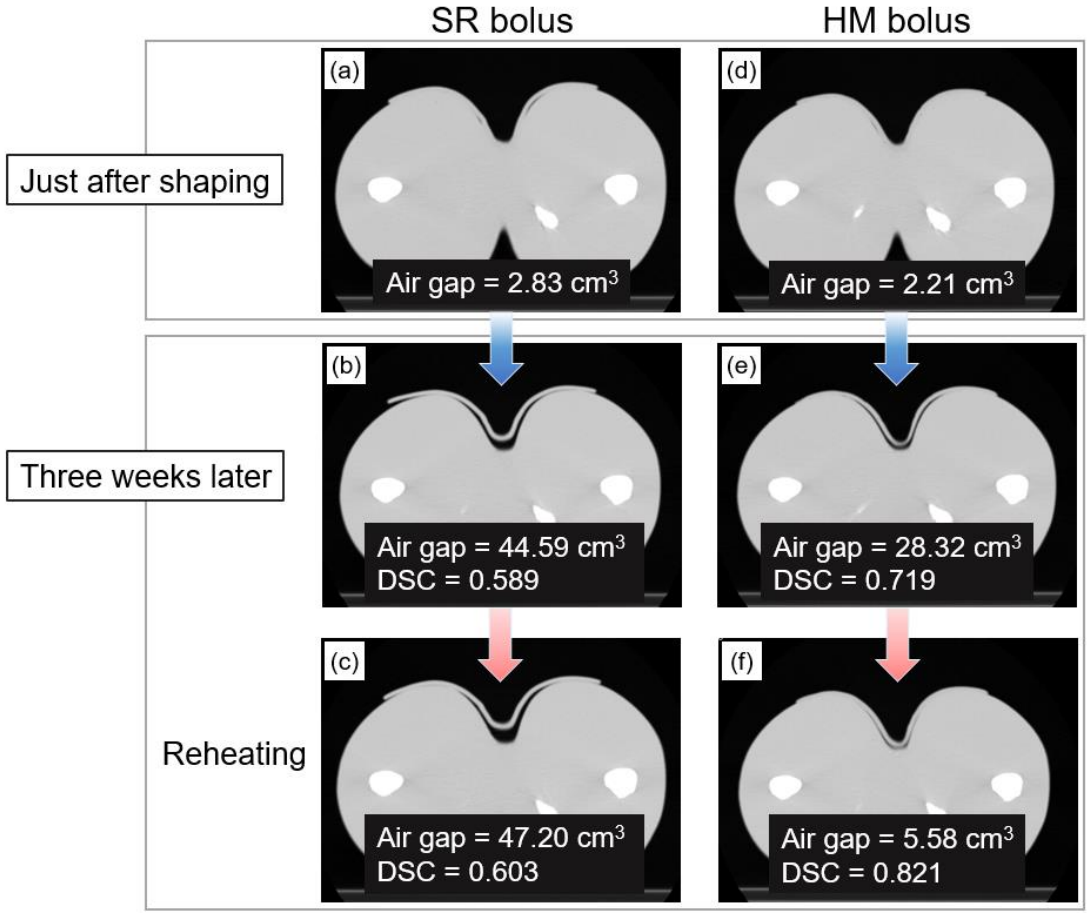

Figure 6. Images of the pelvic phantom with each bolus closely adhered. The SR and HM boluses (a, d) just after shaping, (b, e) left for 3 weeks after shaping, and (c, f) then reheated.

Table 2 shows the air gap and DSC for each bolus just after shaping, and 1, 2, and 3 weeks after shaping. The mean values of the air gap for the Gel bolus, SR bolus, and HM bolus were 96.02 ± 43.77 cm^3, 34.93 ± 21.44 cm^3, and 4.40 ± 1.50 cm^3, respectively. The mean CT value (HU), which indicates density stability, did not change over time for all boluses. The mean DSC values for the Gel bolus, SR bolus, and HM bolus were 0.363 ± 0.035, 0.556 ± 0.042, and 0.837 ± 0.018, respectively. The HM bolus showed the smallest air gap at all time points compared with the Gel bolus and SR bolus. The variation was also the smallest. In addition, the HM bolus showed the best reproducibility with the image just after shaping

when setup again.

Table 2. The air gap, mean CT value and dice similarity coefficient (DSC) for each bolus just after shaping, and 1, 2, and 3 weeks after shaping.

	Just after shaping			One week later			Two weeks later			Three weeks later		
	Gel bolus	SR bolus	HM bolus	Gel bolus	SR bolus	HM bolus	Gel bolus	SR bolus	HM bolus	Gel bolus	SR bolus	HM bolus
Air gap (cm^3)	52.69	2.83	2.21	139.28	45.65	4.84	64.45	44.04	4.98	127.66	47.2	5.58
Mean CT value (HU)	-25	-18	-32	-20	-12	-36	-22	-19	-29	-24	-15	-31
DSC	-	-	-	0.361	0.524	0.832	0.398	0.540	0.857	0.329	0.603	0.821

The letter visibility through the HM bolus and Gel bolus was sufficient, and when the HM bolus was set up on the pelvic phantom, the markers that were completely invisible with the SR bolus were visible (Figure 7).

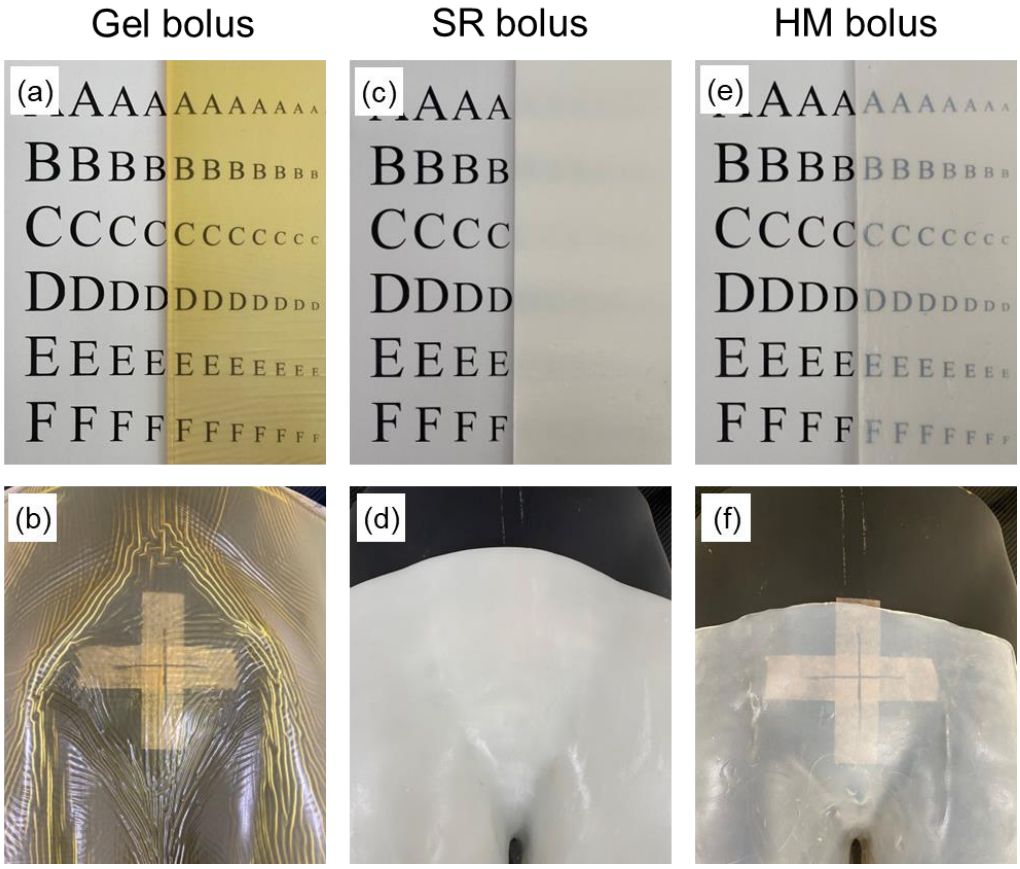

Figure 7. The (a, b) Gel bolus, (c, d) SR bolus, and (e, f) HM bolus placed on letters (maximum: 80 pt, minimum: 10 pt) and markers written on a phantom under normal room lighting conditions.

We developed a HM bolus with unique elasticity and viscosity that can be freely shaped at approximately 40°C and has transparency and temperature dependence. The HM bolus was a tissue-equivalent material from the viewpoint of the atomic number and density. As a result, the HM bolus had the same build-up effect and dose characteristics as a Gel bolus. Therefore, the HM bolus can be used for CT simulation and dose calculation in the same way as a Gel bolus. The high atomic number bolus has advantages over the Gel bolus such as sufficient build-up with a less (thin) material and placement inside the fixture. However, it generates metallic artifacts that prevent accurate dose calculations by TPS (Richmond et al 2016, Al-Rahbi et al 2018, Okuhata et al 2021). Furthermore, a high atomic

number bolus has a significant effect on surface dose enhancement due to backscattering and must be used in consideration of the difference in the interactions with Gel bolus (Richmond et al 2016).

Most previous studies that evaluated bolus adhesion were only conducted at the time of CT simulation and have not been adequately investigated for whether the adhesion at the time of CT simulation can be reproduced after shaping. Malone et al. retrospectively evaluated the adhesion of 3D printed boluses in four different treatment sites of clinical cases over the course of treatment (Malone et al 2022). Their investigation revealed that, compared with the head & neck, scalp, and extremity, only the pelvic case group with vulvar cancer had poor bolus adhesion during treatment. Vulvar cancer is a particularly difficult site to adhere a shaped bolus to during treatment. The virtual bolus technique (Moliner et al 2015) is a method in the treatment plan for vulvar cancer; however, it results in a dose difference from the physical bolus which cannot be used in a completely adherent condition (Fujimoto et al 2017, Park et al 2019, Chatchumnan et al 2022). Furthermore, Chang et al. described the virtual bolus technique as a last resort because it is very time consuming (Chang and Baker 2018). We used the pelvic phantom, assuming vulvar cancer with particularly large unevenness, and shaped it such that the bolus adhered closely from the lower abdomen to the crotch, and evaluated the air gap and DSC. The air gap of the new bolus was the smallest, even 3 weeks after shaping, showing good setup reproducibility. Because the HM bolus showed excellent adhesion to areas that were difficult for a 3D printed bolus to adhere to, the HM bolus is promising for the chest and abdomen, as well as the head & neck, scalp, and extremity.

Park et al. developed a 3D printed bolus using silicon rubber and demonstrated that it could achieve excellent adhesion in clinical cases; however, similar to many other 3D printed boluses, transparency is a disadvantage (Park et al 2019). Muramatsu et al. developed a 3D printed bolus with high transparency and showed the usefulness of being able to setup the bolus while checking its adhesion to the patient's skin (Muramatsu et al 2021). However, the disadvantages of 3D printed boluses are that they take several hours to several days to produce and are not reusable (Canters et al 2016, Fujimoto et al 2017, Baltz et al 2019, Park et al 2019, Muramatsu et al 2021, Chatchumnan et al 2022, Wang et al 2022). The shape memory bolus developed by Aoyama et al. did not have the disadvantages of these 3D printed boluses (Aoyama et al 2020). Furthermore, the bolus could be shaped quickly with adhesion by heating it at 70°C and could be reused by reheating the bolus. One disadvantage is that the 0.15 mm thickness of the material required stacking to obtain sufficient build-up; the HM bolus allows each patient to select the optimal thickness required for build-up.

In a previous study, Wakabayashi et al. developed the SR bolus that can be molded in real time at temperatures greater than 50°C and can maintain their shape at room or body temperature (Wakabayashi et al 2021); however, the SR bolus was a non-transparent material, and they experienced cases in which the adhesiveness of the CT simulation could not be reproduced at each treatment. The free shaping temperature of the SR bolus was 53.0°C, which is greater than that of the HM bolus, and even a short reheat did not sufficiently soften the material. Therefore, the air gap increased after shaping in this adhesion evaluation. Alternatively, the HM bolus can be sufficiently shaped at a lower temperature

(approximately 40°C); therefore, the excellent adhesion can be reproduced every time by reheating the bolus at 60°C for 20 s. The HM bolus could also be easily reused by reheating and returning it to a plate form after use. The HM bolus can be made more viscous with each setup while maintaining its shape in storage, thus allowing it to remain adherent to changes in the patient's body shape during treatment.

The limitation of this study is that data on human skin reactions and allergies to the HM bolus have not been obtained. After clarifying these data, we plan to proceed with clinical trials, including cases in which the product is adapted to patients whose body surfaces change over time.

5. Conclusions

We developed a tissue-equivalent bolus with unique characteristics for clinical use. The advantages of the new bolus are transparency, reusability, and free shaping at approximately 40°C, providing at each setup during the treatment period.

Acknowledgements

This work was supported partly by Japan Society for the Promotion of Science (JSPS) KAKENHI grant number 19K08211. We thank Mr. Masafumi Shigita and Mr. Yoshito Kadowaki for their support. We thank Ashleigh Cooper, PhD, from Edanz (https://jp.edanz.com/ac) for editing a draft of this manuscript.

Conflict of interest

Hajime Monzen received a research donation from Hayakawa Rubber Co., Ltd.

References

Adamson JD, Cooney T, Demehri F, Stalnecker A, Georgas D, Yin FF and Kirkpatrick J 2017 Characterization of Water-Clear Polymeric Gels for Use as Radiotherapy Bolus *Technol. Cancer. Res. Treat.* **16** 923-9

Al-Rahbi ZS, Cutajar DL, Metcalfe P and Rosenfeld AB 2018 Dosimetric effects of brass mesh bolus on skin dose and dose at depth for postmastectomy chest wall irradiation *Phys. Med.* **54** 84-93

Al-Sudani TA, Biasi G, Wilkinson D, Davis JA, Kearnan R, Matar FS, Cutajar DL, Metcalfe P and Rosenfeld AB 2020 eXaSkin: A novel high-density bolus for 6MV X-rays radiotherapy *Phys. Med.* **80** 42-6

Aoyama T, Uto K, Shimizu H, Ebara M, Kitagawa T, Tachibana H, Suzuki K and Kodaira T 2020 Physical and dosimetric characterization of thermoset shape memory bolus developed for radiotherapy *Med. Phys.* **47** 6103-12

Baltz GC, Chi PM, Wong PF, Wang C, Craft DF, Kry SF, Lin SSH, Garden AS, Smith SA and Howell RM 2019 Development and validation of a 3D-printed bolus cap for total scalp irradiation *J. Appl. Clin. Med. Phys.* **20** 89-96

Behrens CF 2006 Dose build-up behind air cavities for Co-60, 4, 6 and 8 MV. Measurements and Monte Carlo simulations *Phys. Med. Biol.* **51** 5937-50

Boman E, Ojala J, Rossi M and Kapanen M 2018 Monte Carlo investigation on the effect of air gap under bolus in post-mastectomy radiotherapy *Phys. Med.* **55** 82-7

Canters RA, Lips IM, Wendling M, Kusters M, van Zeeland M, Gerritsen RM, Poortmans P and Verhoef CG 2016 Clinical implementation of 3D printing in the construction of patient specific bolus for electron beam radiotherapy for non-melanoma skin cancer *Radiother. Oncol.* **121** 148-53

Chang J and Baker J 2018 Consider Using Virtual Bolus *Int. J. Radiat. Oncol. Biol. Phys.* **101** 1027-8

Chatchumnan N, Kingkaew S, Aumnate C and Sanghangthum T 2022 Development and dosimetric verification of 3D customized bolus in head and neck radiotherapy. *J. Radiat. Res.* **63** 428-34

Dice LR 1945 Measures of the amount of ecologic association between species *Ecology* **26** 297-302

Fagerstrom JM 2019 Dosimetric characterization of a rigid, surface-contour-specific thermoplastic bolus material *Med. Dosim*. **44** 401-4

Fujimoto K, Shiinoki T, Yuasa Y, Hanazawa H and Shibuya K 2017 Efficacy of patient-specific bolus created using three-dimensional printing technique in photon radiotherapy *Phys. Med.* **38** 1-9

Geethamma VG, Joseph R and Thomas S 1995 Short coir fiber-reinforced natural rubber composites: Effects of fiber length, orientation, and alkali treatment *J. Appl. Polym. Sci.* **55** 583-94

ICRU 1989 Tissue substitutes in radiation dosimetry and measurement ICRU Report 44 International Commission on Radiation Units and Measurements

Khan FM and Gibbons JP 2014 *Khan's the Physics of Radiation Therapy* (Philadelphia: Lippincott Williams&Wilkins/Wolters Kluwe)

Kong M and Holloway L 2007 An investigation of central axis depth dose distribution perturbation due to an air gap between patient and bolus for electron beams *Australas. Phys. Eng. Sci. Med.* **30** 111-9

Kudchadker RJ, Antolak JA, Morrison WH, Wong PF and Hogstrom KR 2003 Utilization of custom electron bolus in head and neck radiotherapy *J. Appl. Clin. Med. Phys.* **4** 321-33

Lobo D, Banerjee S, Srinivas C, Ravichandran R, Putha SK, Prakash Saxena PU, Reddy S and Sunny J 2020 Influence of Air Gap under Bolus in the Dosimetry of a Clinical 6 MV Photon Beam *J. Med. Phys.* **45** 175-81

Malone C, Gill E, Lott T, Rogerson C, Keogh S, Mousli M, Carroll D, Kelly C, Gaffney J and McClean B 2022 Evaluation of the quality of fit of flexible bolus material created using 3D printing technology *J. Appl. Clin. Med. Phys.* **23** e13490

Moliner G, Izar F, Ferrand R, Bardies M, Ken S and Simon L 2015 Virtual bolus for total body irradiation treated with helical tomotherapy *J. Appl. Clin. Med. Phys.* **16** 164-76

Monzen H, Tamura M, Kijima K, Otsuka M, Matsumoto K, Wakabayashi K, Choi MG, Yoon DK, Doi H, Akiyama H and Nishimura Y 2019 Estimation of radiation shielding ability in electron therapy and brachytherapy with real time variable shape tungsten rubber *Phys. Med.* **66** 29-35

Muramatsu N, Ito S, Hanmura M and Nishimura T 2021 Development of a transparent and flexible patient-specific bolus for total scalp irradiation *Radiol. Phys. Technol*. **14** 82-92

Nakano H, Mishima K, Ueda Y, Matsushita A, Suga H, Miyawaki Y, Mano T, Mori Y and Ueyama Y 2013 A new method for determining the optimal CT threshold for extracting the upper airway *Dentomaxillofac. Radiol.* **42** 26397438

Okuhata K, Tamura M, Monzen H and Nishimura Y 2021 Dosimetric characteristics of a thin bolus made of variable shape tungsten rubber for photon radiotherapy *Phys. Eng. Sci. Med.* **44** 1249-55

Park JM, Son J, An HJ, Kim JH, Wu HG and Kim JI 2019 Bio-compatible patient-specific elastic bolus for clinical implementation *Phys. Med. Biol.* **64** 105006

Recht A, Edge SB, Solin LJ, Robinson DS, Estabrook A, Fine RE, Fleming GF, Formenti S, Hudis C, Kirshner JJ, Krause DA, Kuske RR, Langer AS, Sledge GW Jr, Whelan TJ and

Pfister DG; American Society of Clinical Oncology 2001 Postmastectomy radiotherapy: clinical practice guidelines of the American Society of Clinical Oncology *J. Clin. Oncol.* **19** 1539-69

Richmond ND, Daniel JM, Whitbourn JR and Greenhalgh AD 2016 Dosimetric characteristics of brass mesh as bolus under megavoltage photon irradiation *Br. J. Radiol.* **89** 20150796

Sakai Y, Tanooka M, Okada W, Sano K, Nakamura K, Shibata M, Ueda Y, Mizuno H and Tanaka M 2021 Characteristics of a bolus created using thermoplastic sheets for postmastectomy radiation therapy *Radiol. Phys. Technol*. **14** 179-85

Sharma SC and Johnson MW 1993 Surface dose perturbation due to air gap between patient and bolus for electron beams *Med. Phys.* **20** 377-8

Vyas V, Palmer L, Mudge R, Jiang R, Fleck A, Schaly B, Osei E and Charland P 2013 On bolus for megavoltage photon and electron radiation therapy *Med. Dosim*. **38** 268-73

Wakabayashi K, Monzen H, Tamura M, Takei Y, Okuhata K, Anami S, Doi H and Nishimura Y 2021 A novel real-time shapeable soft rubber bolus for clinical use in electron radiotherapy *Phys. Med. Biol.* **66** 185013

Wang KM, Rickards AJ, Bingham T, Tward JD and Price RG 2022 Technical note: Evaluation of a silicone-based custom bolus for radiation therapy of a superficial pelvic tumor *J. Appl. Clin. Med. Phys.* **23** e13538